IEEE Access
Multidisciplinary | Rapid Review | Open Access Journal

Received March 20, 2019, accepted April 4, 2019, date of publication April 17, 2019, date of current version May 31, 2019.

Digital Object Identifier 10.1109/ACCESS.2019.2911454

A Bio-Fuel Power Generation System With Hybrid Energy Storage Under a Dynamic Programming Operation Strategy

XIANG-PING CHEN[1,2], (Member, IEEE), YAO-DONG WANG[3], AND QIN-MU WU[1]

[1]School of Electrical Engineering, Guizhou University, Guiyang 550025, China
[2]School of Engineering, Cardiff University, Cardiff CF10 3AA, U.K.
[3]Sir Joseph Swan Centre for Energy Research, Newcastle University, Newcastle upon Tyne NE1 7RU, U.K.

Corresponding author: Qin-Mu Wu (ee.xpchen@gzu.edu.cn)

This work was supported in part by the EU H2020 Project TowArds Building rEady for Demand rEsponse (TABEDE) under Grant 766733, and in part by the National Natural Science Foundation of China (NSFC) under Grant 51867007, Grant 51867006, and Grant 51867005.

ABSTRACT This paper proposes a dynamic programming (DP)-based operational strategy for a biofuel distributed generation system with hybrid energy storage (BDG-HES). The proposed system consists of a biofuel-powered engine and a gen-set, six battery packs, a super-capacitor module, and four power electronic converters. It is primarily designed to meet the electrical demand of a typical UK family while the energy storage system can reduce the operating duration of the engine so as to improve the fuel efficiency. The DP, as an optimization strategy, is used to determine the operational scheme for the BDG-HES. In this paper, four case studies are carried out based on real-world measurement data. The test results have confirmed the effectiveness of the proposed methodology. The overall system efficiency is improved by approximately 19% over the operational range compared to a conventional gen-set based power system.

INDEX TERMS Biofuel, distributed generation, dynamic programming, gen-set, hybrid energy storage, optimal operation.

I. INTRODUCTION

The past decades have seen a rapid development of distributed generation (DG) systems due to increasing penetration of renewable energy into the power network, including wind, solar and bio-energy [1], [2]. In the UK, renewables from wind, solar, hydro and biofuel account for 26.6% of the total electricity generation [3]. Remarkably, bioenergy is a major contributor to renewable power generation, representing 36% of the total, as shown in Fig. 1. For distributed generation (DG) research and applications, most of them are at a district level which supplying electricity to a community [4]–[6] while household level power demand is much more fluctuated and have not been studied in the past. Conventionally, a gen-set is needed to operate 24 hours to meet the demands while loads fluctuate over the duration. The gen-set in the DG would have to run continuously at high or low loads all the time. But the gen-set driven by internal combustion engines (ICEs) can achieve high efficiency only at high load [7]. Operating at low loads (<50% of engine full-load) will significantly reduce engine efficiency. Presently, biofuel-based power systems are being researched only in laboratories while their industrial applications are hampered by low system efficiency and high cost. In order to address these issues, an effective energy storage system and an optimized operational scheme are needed to schedule the operational events and to manage power flow between the different components. From our previous study [8], it was found that typical household energy consumption can be separated into three ranges: the power below 0.5 kW is for 68% of the day; 0.5-10 kW for 29%; and the power above 10 kW for 3% of the day. The average power consumption is around 1.5 kW per hour in a typical day in winter. If a gen-set was used alone to supply the power, the overall efficiency would be very low. Therefore, a hybrid energy storage (HES) is necessary to store a certain amount of electricity during the off-peak hours and then output it during peak hours. The advantage of using the HES (batteries with supercapacitors) is that the electrical energy from the supercapacitor is discharged first followed by the battery, i.e. the supercapacitor releases its stored energy faster than the

The associate editor coordinating the review of this manuscript and approving it for publication was Nishad Mendis.

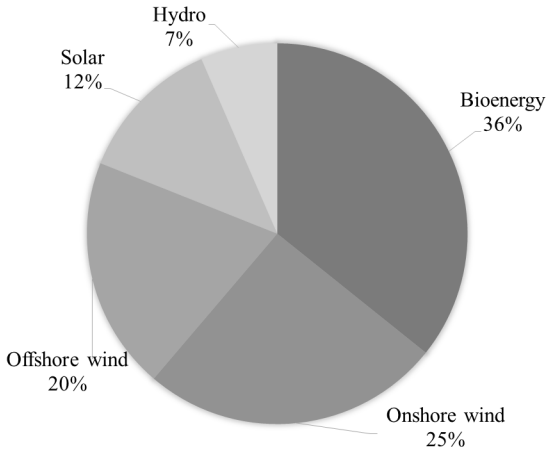

FIGURE 1. Electricity generation from renewables in 2016 [3].

battery, specifically are used to meet the short-term demand and the battery for longer term demand. This means that the supercapacitor responds to the load quickly so that it reduces stress on the battery [8]. From this study, it was also found a necessity for developing a proper operation strategy for the DG-HES system in order to achieve a high efficiency of the engine.

DG can be selected and evaluated by using an adapted stochastic framework to obtain the optimal allocation and timing of renewable distributed wind and solar PV generations to minimize the costs, in presence of uncertainties of generation, load demands and tariff variations [9]. The stochastic method can be used for controlling the costs of renewable energy systems, a combine heat and power (CHP) system, and variable loads [10]; and for a DG with an additional battery energy storage system [11]. The method addresses uncertainties in demand, component failure and weather changes, but it is complicated and has a high computational requirement. The method is mainly used at the design stage or modelling of the systems.

Reference [12] studied an integration of PV, fuel cell (FC) and ultra-capacitor (UC) system for stand-alone applications by modelling. The operation strategy was set as follows: when PV could not meet the load demand, the FC provides power to aid it. If the demand increased to surpass the FC capability, the UC bank is started to work. Reference [13] performed an experimental study in laboratory, using their hybrid system including PV panels, wind generator and biomass gasification plant, plus a battery bank for energy storage, to verify the reliability and feasibility of hybrid renewable systems. Their control strategy is set up according to battery charge status: when it was down to 50% of its nominal full charge, the biomass gasification plant started to work. They found that such a strategy could operate the whole system well to meet the demand. Reference [14] designed, implemented and tested a hybrid syngas/solar PV/battery power system for off-grid applications. From the actual tests, the hybrid solar PV/battery system with a standby syngas genset was running more stable and reliable to meet the dynamic power demand than that without the genset. The operation strategy of their genset was set according to the state of charge (SOC) of the batteries. The gen-set is automatically switched on when SOC drops to 40% and switched off when the SOC reaches 80%. Reference [15] developed optimization concept of SOC and minimum costs for the design and operation of hybrid PV-engine system. A study in reference [16] presented the operation results of their combined PV, wind and bio-gas genset to power the sewage plant on the island of Fehmarl, Germany, but they did not explain what operation strategy was used. The operations of the above systems were not designed for optimal operation.

These reported existing operating methods are effective for relatively large distributed systems and large loads and for long durations (in hours) [4]–[6] [17]–[20]. However, it is more challenging to operate a micro/mini power system for a household where the demand can change from hundreds of watts to over tens of kilowatts quickly.

This paper is focused on a bio-fuel powered power system with hybrid energy storage (HES) for household applications. A new operational method is proposed to improve the system energy efficiency. The work attempts to match the changing loads with the biofuel distributed generation (BDG) system and the HES based on DP optimization method. System state variables, operational variables and the objective function are defined under the DP framework. A decision tree is developed to solve the optimization problem so as to control the power flow between different components in the system. The technology developed in this study overcomes the drawbacks of conversional ICE-based power generation when it is used in domestic applications. By comparing to a conversional system, it has been confirmed that both the energy efficiency and operational durations are improved in this BDG-HES system.

II. PRINCIPLE OF OPERATION

The proposed system consists of a bio-diesel engine, a gen-set, six batteries, a supercapacitor module and power converters. The bio-diesel engine is fed with liquid biofuel which is preheated to a high temperature (90°C in this case). Heating is extracted from the engine and the exhaust gas. The diesel engine is only operated at optimized durations to generate electricity.

Conventionally, the diesel engine is operated continuously to meet the fluctuating demand. In this system, it is only operated at optimized conditions for power generation so that the engine's operational duration is reduced dramatically. Six Gel batteries and a supercapacitor module are used to form an energy storage system to meet the peak demand. Once the engine is running, the gen-set connected to the engine to yield single-phase 230V alternative current (AC) power. AC power is first rectified into direct current (DC) power and then reduced to a 24V DC power to supply the DC link. This DC bus is connected to the load, batteries and supercapacitors

in order to supply power to the load via an inverter. Electrical power flow in the batteries and supercapacitors are two-directional (charging and discharging).

A. ENGINE PERFORMANCE WITH BIO-FUELS

In the tests, the engine is fed by four vegetable oils (bio-fuels), which are croton oil, jatropha oil, rapeseed oil, and sunflower oil. The viscosity of raw vegetable oils is higher than that of diesel fuel which would slow down the combustion process if used directly. Therefore, they are preheated before combustion. Fig. 2 shows the viscosity of fuels as a function of their temperature. As can be seen, the viscosity of these oils drops to approximately 3 mPa.s when heated to 120°, which is comparable or better than that of the diesel of 3.0 mPa.s at 30 ° (benchmark).

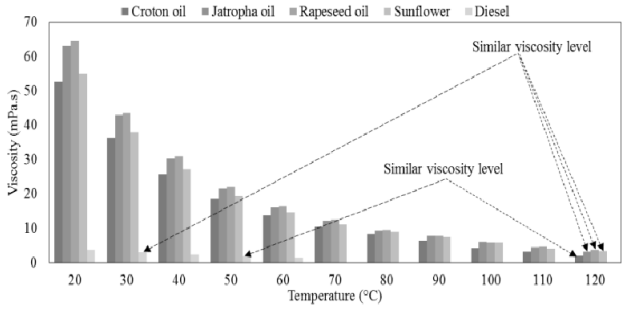

FIGURE 2. Fuel viscosity as a function of the temperature.

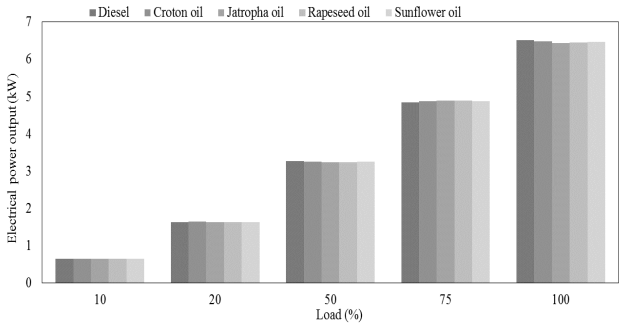

FIGURE 3. Engine output power powered by different fuels.

Fig. 3 demonstrates the engine/generator performance using the four preheated vegetable oils (to 90°). The reference electrical loads are 0.65 kW, 1.625 kW, 3.25 kW, 4.875 kW and 6.5 kW, corresponding to 10%, 25%, 50%, 75% and 100% loads, respectively. The results show the power output increase with the load nearly proportionally. The difference in output powers from four biofuels is fairly small. This proves the feasibility of utilizing these biofuels in the CHP engine in place of diesel.

Fig. 4 demonstrates the electrical efficiency when different fuels are used. The engine with these fuels presents similar electrical efficiency under the same load ratio. Diesel is the best performer among all fuels under all load conditions.

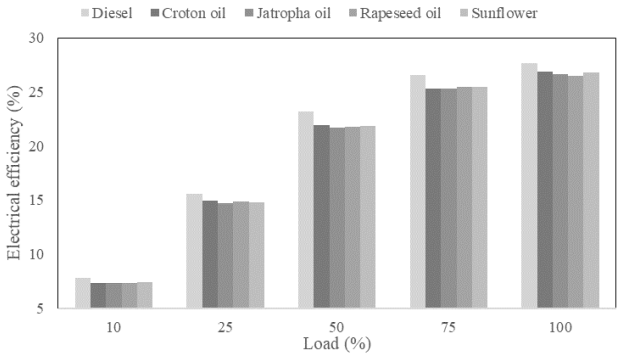

FIGURE 4. Engine electrical efficiency by different fuels.

On the other hand, all the fuels demonstrate that the electrical efficiency grows with the increase of the load ratio. When the load ratio promotes over 50%, the efficiency raises a lot from 21.9% to 27.7%. Otherwise, the efficiency is lower than 15% for all the fuels. The experimental results shown in Fig. 4 indicate that a bio-fuel engine and an associated generator play preferable performance when the load ratio is higher than 50%. Therefore, a biofuel engine working under relatively high load will promote its performance which in turn improve the overall efficiency of the whole system proposed.

B. HES

In the proposed system as illustrated in Fig. 5, the gen-set supplies the base load while the HES meets the peak demand and other demands when the engine is not operated. Especially for the super-capacitor module, a wide voltage range is desired for storing energy, requiring the use of a buck-boost DC/DC converter to interface with the load.

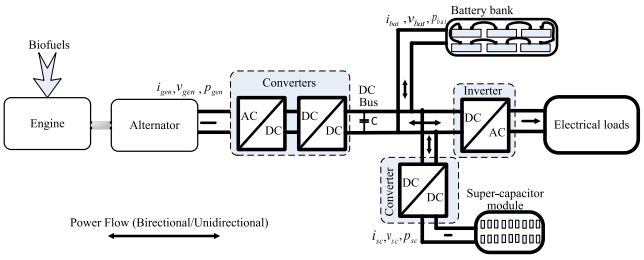

FIGURE 5. Schematic diagram of the proposed system.

In this study, the liquid gel batteries are the main component to store electrical energy in the system in order to balance the supply and demand. Similar to lead acid batteries, their performance is dependent on polarization. On the one hand, the batteries suffer from power loss (heat) during the discharging process. The severe degree depends on the voltage and the discharging current. On the other hand, their equivalent resistance will rise with the voltage or current [21], [22].

Compared to the batteries, super-capacitors can store less electrical energy but provide much faster response to demand

changes. The life cycle of supercapacitors can easily exceed 1 million times. The stored energy in a super-capacitor is proportional to the capacitance and the terminal voltage squared. As a result, an increase in the voltage is more significant than the increase in the capacitance in energy storage.

III. DYNAMIC PROGRAMMING FOR ENERGY MANAGEMENT

DP is both an optimization algorithm and a programming tool. It is reported in use in multi-source energy systems [23]–[26]. In general, DP can model nonlinear dynamics with constraints by discretizing the state and decision variables with respect to time. Each state which includes one or multi components (variables) is used to form an objective value. The calculation stages interact and interconnect with decision (or control) variables. In essence, the target of DP is to find the best decision set over the whole searching trajectory.

A. DYNAMIC PROGRAMMING AND THE TARGET

The idea behind the DP optimization is as follows. Suppose State (k) is a current state. It should take a decision/control variable into account to generate the next state, namely, State (k + 1). In this case, a decision/control selection is aimed to find the best candidate for energy efficiency over the search trajectory at each stage.

The energy management is based on the power balance between demand and supply at any time

$$p_{bat}(t) + p_{sc}(t) + p_{gen}(t) = p_{load}(t) \tag{1}$$

where $p_{gen}, p_{load}, P_{bat}, p_{sc}$ refer to the power from the gen-set, load, batteries and supercapacitors, respectively. For batteries and supercapacitors, a positive power value represents discharging and a negative value for charging. The energy management process is demonstrated in the flowchart in Fig. 6.

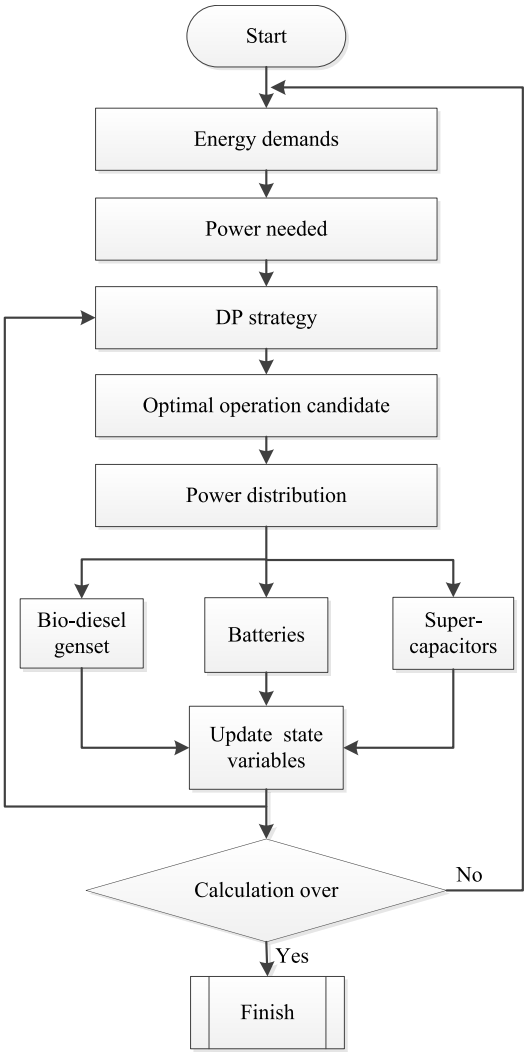

FIGURE 6. Flow chart of the energy management in the BDG-HES.

B. OPTIMIZATION PROCESS

In the optimization, there are three components used as the control vectors: gen-set, batteries and supercapacitor. For the sake of simplicity, batteries and supercapacitors are grouped, and their power and energy are defined as p_{st} (t) and E_st(t), respectively. Eq. 1 can be rewritten as,

$$p_{gen}(t) + p_{st}(t) - p_{load}(t) = 0 \tag{2}$$

There are one state variable and two control variables for the optimization problem. At each stage, the state variable refers to the SOC of the HES. This term is given by:

$$s(t) = \frac{1}{Q_{st}} \int_0^t i_{st}(t)\, dt + soc_{st}^0 \tag{3}$$

where Q_{st} and soc_{st}^0 refer to the capacity constant and initial SOC of HES. The power from the gen-set and HES are selected as two control variables in the optimization. Then,

$$x_1(t) = p_{gen}(t) \tag{4}$$

$$x_2(t) = p_{st}(t) \tag{5}$$

Therefore, we can construct the control variable sequence as $X(t) = [x_1(t), x_2(t)]$.

When applying DP to any problem, we can transfer a time-continuous problem into a time-discrete problem. State variables and control variables are redefined by their discrete formations. At time instant k = 1, 2 . . .,

$$x_1(k) = p_{gen}(k) \tag{6}$$

$$x_2(k) = p_{st}(k) \tag{7}$$

Then

$$X(k) = [x_1(k), x_2(k)] \tag{8}$$

Meanwhile,

$$s(k) = \frac{1}{Q_{st}} \sum_{j=1}^{k} i_{st}(j) + soc_{st}^0$$

$$= \frac{1}{Q_{st}}(\sum_{j=1}^{k-1} i_{st}(j) + i_{st}(k)) + soc_{st}^{0}$$
$$= \frac{1}{Q_{st}} \sum_{j=1}^{k-1} i_{st}(j) + \frac{1}{Q_{st}} * i_{st}(k) + soc_{st}^{0} \quad (9)$$

Assuming the DC voltage of the energy storage system is constant, $i_{st} = \frac{p_{st}}{v_{st}}$ and $m_0 = \frac{1}{Q_{st} * v_{st}}$, then

$$s(k) = s(k-1) + m_0 * x_2(k) \quad (10)$$

The state transmission function can be derived as follows,

$$x_1(k+1) + x_2(k+1) = p_{load}(k+1) \quad (11)$$
$$s(k+1) = F(s(k), X(k), k) \quad (12)$$
$$(s(k), X(k), k) = s(k) + m_0 * x_2(k+1) \quad (13)$$

The objective function can be listed as follows:

$$J(S(0), x(0), 0) = \sum_{k=0}^{\infty} m_1 \left(\frac{x_1(k)}{p_{nom}} - 1\right)^2 + m_2 \left(\frac{x_2(k)}{p_{st}^{0}}\right)^2 + m_3 (s(k) - 1)^2 \quad (14)$$

where parameters p_{nom} and p_{st}^{0} refer to the nominal power of the gen-set and the nominal discharge power of the HES. Three coefficients m_1, m_2, m_3 are the weight factors in the calculations. The physical meaning behind the objective function includes three parts. The first term is related to the output power from the gen-set. The engine/gen-set is expected to operate at relatively high level for high efficiency. The closer to the nominal power of the gen-set, the better is the engine performance. The second term is related to the power level of the HES. Battery discharge/charge at the nominal discharge/charge power benefits to the life-cycle of the HES and system efficiency [27], [28]. The third part represents the close level to the full SOC of the HES which guarantees sufficient energy in the storage system.

The control variable space is defined as

$$\mathbb{X}_k = \{X_0(k), X_1(k), X_2(k), X_i(k) \in \mathbb{R}, i = 0, 1, \ldots\} \quad (15)$$

The optimization function is written as follows,

$$J^*(s(k), X(k), k) = \inf_{X_i(k)} \{J(s(k), X_i(k), t) : X_i(k) \in \mathbb{X}_k\} \quad (16)$$

Let

$$\mathrm{P}(s(k), X(k), k) = m_1 \left(\frac{x_1(k)}{p_{nom}} - 1\right)^2 + m_2 \left(\frac{x_2(k)}{p_{st}^{0}}\right)^2 + m_3 (s(k) - 1)^2 \quad (17)$$

Then, a discrete-time Bellman equation is obtained by

$$J^*(s(k), X(k), k) = \min_{X_i(k)} \{P(s(k), X_i(k), k) + J^*(s(k+1) + X(k+1), k+1)\} \quad (18)$$

C. DECISION TREE AND DP SOLUTION

In general, it is difficult to obtain an optimal control sequence by direct iterations from the objective equation. Considering electrical demands in this study, they can be divided into three categories: low demand, off-peak demand and high demand for each time slot. For each operational candidate, four options could be found. A decision tree is thus employed to solve the optimization problem instead of using iteration calculations in this work which is also used by reference [29]. Fig. 7 illustrates the decision tree where an optimal decision search at each stage is developed accordingly.

There are two decision/control variables at each time instant. Therefore, two variables with four possible combination are available, namely, running engine with discharging the HES, running engine with charging the HES, solely discharging the HES, and solely running engine. These options as recorded as d_1, d_2, d_3, d_4.

There are two levels of decision nodes. The first level decision nodes include 4 options. The second level includes 12 nodes with 2 possible options for each node (satisfied, unsatisfied). Also, 2 level outcome nodes are needed in the process. Each outcome node contains parameter $\xi_{i,j}$ and the last outcome nodes receive the value v_m where $\xi_{i,j}$ and v_m stand for a possibility degree at level i with route j, and the profit at the end nod, respectively. For instance, parameter $\xi_{1,2}$ places on node level 1. In this case, the possibility of the engine load ratio with SOC_{HES} 100% is $\xi_{1,2}$.

From the decision tree, an optimal decision candidate is selected on the basis of its maximum contribution value of the route. For instance, at some stage, the demand goes high where the engine load is 95% and the HES is fully charged. Therefore the possibility coefficient vector are obtained as follows,

$$\xi_{1,\mathrm{j}_{\mathrm{j}=1\sim4}} = \{0.5, 0.3, 0.1, 0.1\} \quad (19)$$
$$\xi_{2,\mathrm{k}_{\mathrm{k}=1\sim12}} = \{1, 0, 0, 0, 1, 0, 0, 0, 1, 0, 1, 0\} \quad (20)$$
$$\xi_{3,\mathrm{l}_{\mathrm{l}=1\sim24}} = \{0.6, 0.4, 0.5, 0.5, 0.5, 0.5, 0.5, 0.5, 0.4, 0.6, 0.5, 0.5, 0.5, 0.5, 0.5, 0.5, \ldots.0.6, 0.4, 0.5, 0.5, 0.6, 0.4, 0.5, 0.5\} \quad (21)$$
$$v_{m_{(m=1\sim24)}} = \{0.8, 0.6, 0.4, 0.3, 0.2, 0.1, 0.1, 0.1, 0.8, 0.6, 0.4, 0.3, 0.2, 0.1, 0.1, 0.1, 0.8, 0.6, 0.4, 0.3, 0.8, 0.6, 0.4, 0.2\} \quad (22)$$

Vectors are given by:

$$\mathrm{out}_{\mathrm{m}_{(\mathrm{m}=1\sim24)}} = \{0.24, 0.12, 0, 0, 0, 0, 0, 0, 0.096, 0.108, 0, 0. \ldots, 0.048, 0.024, 0, 0, 0.012, 0.004, 0, 0\} \quad (23)$$

The maximum value of the outcome vector is 0.24 and therefore the optimal decision d_1 is selected by backward derivation.

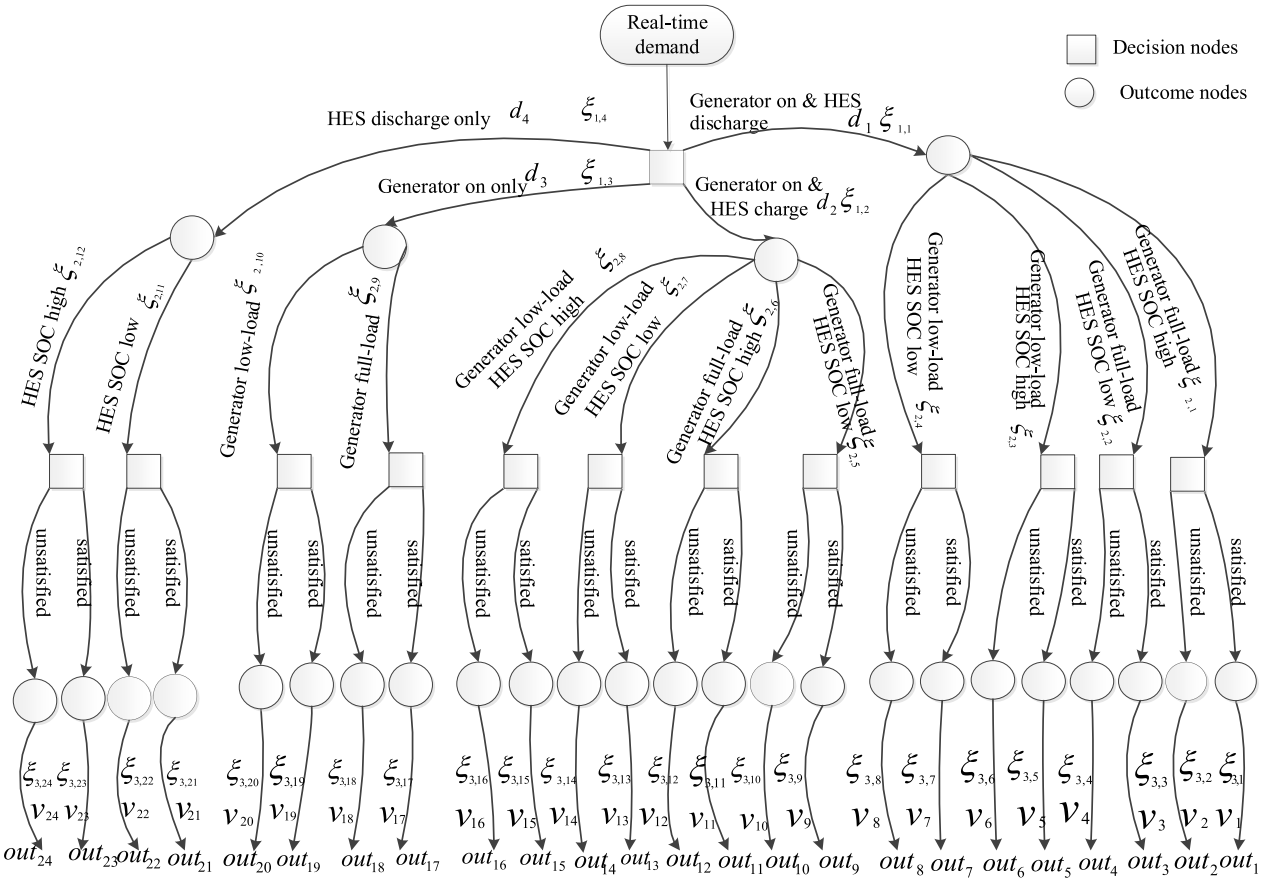

FIGURE 7. Decision tree in an optimal trajectory [29].

IV. RESULTS AND ANALYSIS

The target household is a semi-detached two bed-room house which is typical family home [30].

A. SOCIAL AND DEMOGRAPHIC CHARACTERISTICS OF THE OCCUPANTS

In order to understand the domestic energy needs, the social and demographic characteristics of the occupants are recorded. Measured data are summarised in Table I.

The family has a quite similar activity pattern each day. The activity pattern can be generally divided into morning section, mid-day section and evening section. For instance, from 7:00 to 9:30 in spring, the occupants carry on different activities which give rise to the variation of energy consumption. The morning section starts earlier in the summer at 5:30. The midday section is from 11:00 to 14:00 in winter which is slightly earlier than that in summer since occupants might come back home earlier in winter due to cold weather.

Table II lists the statistic results for appliance usage in this house. The appliances are divided into four categorizes according to their usage purposes. Appliances in the bedrooms mainly include electronic device such as mobile charger, game paddles, etc.; living room has appliances such as desktops, TV, printers, vacuum cleaner; kitchen has appliances with high energy consumption, including microwave, oven, cooker, kettle, wash machine, dish washer, etc.; lighting takes up a quite large percent of energy consumption in the house. It consumes more energy in spring and winter since less natural light in these seasons needs more electricity to increase illuminance over the day. Also, energy consumption pattern in weekday is different with that in weekend or holidays. Therefore, occupants schedule and appliances usages are divided into weekday group and weekend/holiday group accordingly. As can be seen from Table 3, the usage time of the appliances are summarized with these four categories.

B. DEMAND PROFILES IN CASE STUDIES

In this study, the DP is designed to deal with the supply-side power management, namely, to meet the demand using various sources. It would be useful to examine load profiles under different scenarios. Different daily electricity consumption modes in four seasons are investigated to validate satisfaction of the proposed methods. The key features of power and energy needs are summarized in Table III while the waveforms in Fig. 8 display the dynamic scenarios of the demands in these days.

As can be seen in Table III, the power range in different season day are diverse. The spring day is from 0 to 5.8kW

TABLE 1. Occupancy schedule.

Week days				Weekends/Holidays			
Jan-Mar	Apr-Jun	July-Sep	Oct-Dec	Jan-Mar	Apr-Jun	July-Sep	Oct-Dec
07:00-09:30 13:00-15:00 16:30-22:00	05:30-09:30 13:00-14:00 16:00-22:00	06:30-09:30 12:00-14:00 16:00-22:00	07:00-09:30 11:00-15:00 16:00-22:00	09:00-17:00 19:00-24:00	09:00-17:00 19:00-01:00	09:00-17:00 19:00-01:00	09:00-17:00 19:00-01:00

TABLE 2. Usage scenarios of electrical appliances.

	Week days				Weekends/Holidays			
Category	Jan-Mar	Apr-Jun	July-Sep	Oct-Dec	Jan-Mar	Apr-Jun	July-Sep	Oct-Dec
Electronic devices (bedroom)	0:30-06:30	0:30-04:30	0:30-04:30	0:30-06:30	0:30-06:30	0:30-04:30	0:30-04:30	0:30-06:30
Catering	07:00-09:00; 18:00-20:00	07:00-09:00; 18:00-20:00	07:00-09:00; 18:00-20:00	07:00-09:00; 18:00-20:00	07:00-09:00; 18:00-20:00	07:00-09:00; 18:00-20:00	07:00-09:00; 18:00-20:00	07:00-09:00; 18:00-20:00
Lighting	0:30-01:00; 06:30-09:30; 17:00-23:00	0:30-02:00; 19:00-23:00	0:30-02:00; 20:00-23:00	0:30-01:30; 06:00-09:00; 16:30-23:00	0:30-01:00; 06:30-9:30; 17:00-3:00	0:30-02:00; 19:00-23:00	0:30-02:00; 20:00-23:00	0:30-01:30; 06:00-09:00; 16:30-23:00
Living room	8:00-22:00	8:00-22:00	8:00-22:00	8:00-22:00	8:00-24:00	8:00-24:00	8:00-24:00	8:00-24:00

TABLE 3. Daily consumption in 4 chosen days.

Key indicator	27th March	22nd June	19th September	4th December
Power range of the demand (kW)	0 - 5.8	0 - 6.1	0 - 9.7	0 - 8.9
Daily electrical consumption (kWh)	12.0	11.1	16.1	12.5
Period of low demand (hrs)	22.4	22.2	21.4	21.4
Period of peak demand (hrs)	0.12	0.12	0.23	0.23
Low demand percentage (%)	93.3	92.5	89.2	89.2
High demand percentage (%)	0.5	0.5	0.96	0.96

while the upper power limit raises to 9.7kW in the autumn day since more kitchen appliances are needed in that morning. The Autumn day consumes the most energy (16.1kWh) over the rest three days, which may be caused by the longer period of washing machine usage and cooking activities. The Winter day also consumes pretty much energy over the spring and the summer days. In terms of the period and the percentage of the low demand, four season days display similarity. However, the period and percentage of high demand are double in autumn and winter days compared to the counterparts in the spring and summer days.

In Fig. 8, it can be seen that the demands fluctuate from time to time and have both low (dozens of watts) and peak hours (several thousand watts) over the evaluated periods. The peak demands in both autumn and winter days are higher than those in spring and summer days.

Four typical days show a similar trend that the peak hours were less than 1 hour even in autumn and winter days. In any of these 4 days, lower demands (below 1kW) are found in the majority of 24 hours.

Power consumption scenarios in Fig. 8 can also be seen as three zones in each day which is compatible with the categories of morning section, midday section and evening section as discussed above. Take the spring day for instance, the consumption increases dramatically from 6:30 in the morning which reaches the peak at 8:15. Afterwards, the consumption fluctuates before decreasing to lower than 1kW. From 13:00, the consumption increases again till 14:00. In this midday section, energy consumption also fluctuates due to different appliances are used over this period. 17:00 sees more energy consumption again. Afterwards, a new peak appears around 19:00. Three sections are less appar-

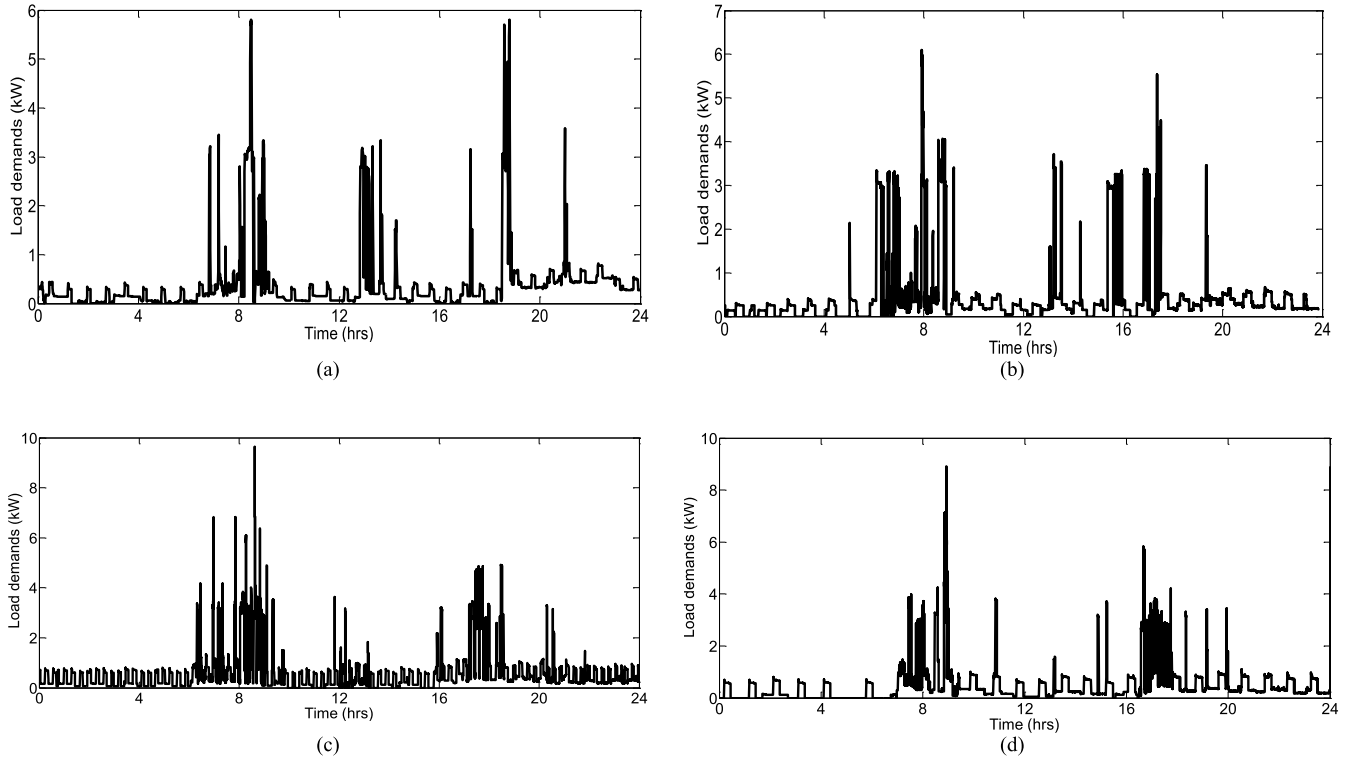

FIGURE 8. Typical days for domestic electricity consumptions over four seasons [20]. (a) Spring day; (b) Summer day; (c) Autumn day; (d) Winter day.

TABLE 4. Specifications of the BDG-HES.

Engine		Gen-set		Battery		Super capacitor	
Type	Yanmar TF120M	Model	YTG6.5S	Type	Gel batteries	Cell	1000 F/2.7 V
Speed	2400 rpm	Gen-set	MR2-160/2	No. of units	6	unit	24
Cooling system	radiator	Capacity	6.5 kVA/6.5 kW	voltage	12 V	capacity	40 F
Continuous power output	7.72 kW	Current output	29.5 A	Capacity/unit	120 Ah	voltage	60 V

ently divided in the selected winter day since that day is a weekend and the occupants have a lightly different activity schedule from the weekday.

C. SYSTEM MODELLING

After analysis the consumption features of the house. The specifications of power components are selected. First of all, the power range is within 10kW and low consumption (lower than 1kW) are requested over the most day (around 21 hours) in the selected days. Therefore, the genset with 6.5kW power range is selected where biodiesel engine Yanmar TF120M with continues mechanical power of 7.72kW is linked with the genset. Since there are 3.2kW power discrepancy between the peak demand and genset output power, energy storage consisting 6 units of battery (120Ah/12V per unit) and supercapacitors (60V/40F) are used to provide extra assistance in peak period. The detailed specification of the power components in the BDG-HES system is tabulated in Table IV.

This investigation employs modelling/simulation platform Modelica/Dymola to implement the system where the model parameters refer to the outcomes of the previous investigations [8], [31] on the basis of physical systems and preliminary tests. The input data are obtained from actual measurement where the proposed methodology is tested in simulation. Dymola refers to the ''Dynamic Modelling Laboratory'' which is suitable for modelling multidisciplinary, complex physical systems, including mechanical, electrical, thermodynamic, hydraulic, pneumatic, thermal and controlling system [32], [33].

D. ENERGY EFFICIENCY

Generally, energy efficiency can be calculated by:

$$\eta = \frac{Energy\ output}{Energy\ input}$$

or

$$\eta = \frac{Power\ output}{Power\ input} \tag{24}$$

The biofuel consumption, equivalent energy amount of the bio-engine, equivalent power input/output of the bio-engine are investigated by experimental test data. Efficiency

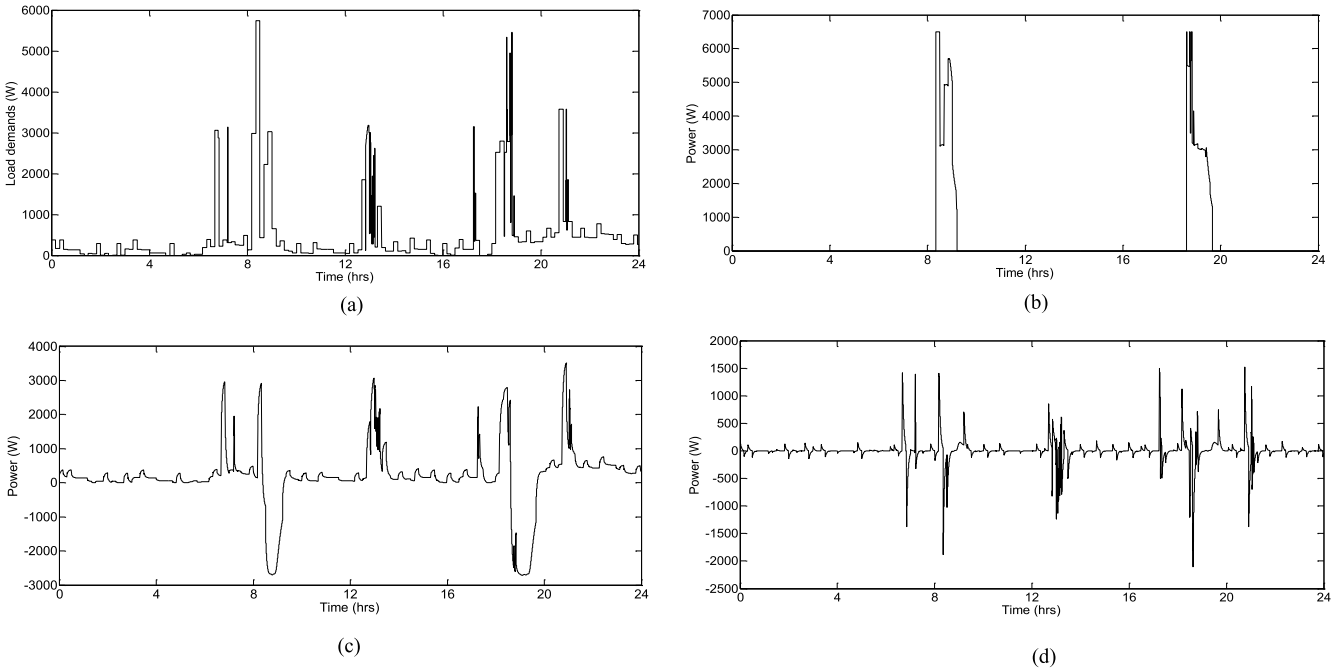

FIGURE 9. Demands and supply for one spring day in case studies. (a) load demands over 24 hours, (b) power profile of the gen-set, (c) power profile of the batteries, and (d) power profile of the supercapacitors.

calculations in this study employ the outcomes, including $\xi_{eng}(t, p_{elec})$ (engine efficiency versus power output), $\xi_{ch}(t, p_{elec})$ (HES charge efficiency versus power input), $\xi_{\frac{ch}{disch}}(t, p_{elec})$ (efficiency via charge/discharge).

The engine electrical efficiency refers to the mean efficiency over its operational duration. Let $\xi_{eng}(t, p_{elec})$ be the real-time electric efficiency at engine output power p_{elec}. The overall efficiency is an integration of the efficiency at the engine duty time $\{T_1, T_2, \ldots T_K\}$. So the overall efficiency is calculated by:

$$\eta_{eng} = \frac{\int_0^K \left[\int_0^{T_i} \xi_{eng}(t, p_{elec})\, dt\right] T_i di}{\int_0^K T_i di} \tag{25}$$

By considering the power loss in both charging and discharging processes, the HES efficiency η_{HES} is equal to its mean charge efficiency $\eta_{ch}(t)$ times its transferring efficiency from charging to discharging $\xi_{\frac{ch}{disch}}(t, p_{elec})$. The electrical efficiency η_{HES} can be expressed as

$$\eta_{HES} = \frac{\int_0^K \left[\int_0^{T_i} \eta_{ch}(t) \times \xi_{\frac{ch}{disch}}(t, p_{slec})\, dt\right] di}{\int_0^K T_i di} \tag{26}$$

$$\eta_{ch}(i) = \frac{\int_0^{T_i} \xi_{ch}(t, p_{elec})\, dt}{T_i} \tag{27}$$

By integrating the efficiency of the each component with respect to the operational time, the overall system efficiency η_{st} can be calculated by:

$$\eta_{st} = \frac{\eta_{eng} \times T_{eng} + \eta_{HES} \times T_{HES} + 0.5 \times (\eta_{eng} + \eta_{HES}) \times T_{tgt}}{T_{eng} + T_{HES} + T_{tgt}} \tag{28}$$

E. ANALYSIS AND DISCUSSION

Fig. 9 shows demand and supply profiles in the case studies. Power variations following the demands fluctuation are expected. Even though the peak power is different among these four days, the maximum outputs from the energy sources kept same level.

As can be seen in Fig. 9(a), peak hour starts from 8:15, the majority electrical power come from the gen-set (6.5 kW) where extra power is provided by the HES to meet the demand. Low or medium level of the energy demands in the most day are satisfied by the HES while the genset runs only two period of times in the day. It deserves to be noticed that even the peak hour in the evening around 5.5 kW. The genset contributes the maximum power with 6.5 kW to the system at the same time where 1 kW is used to charge the HES. Afterwards, the genset keeps running with decrease output until 19:40 as the HES is fully charged.

The positive value of the waveforms in Figs. 9(c) and (d) stands for the discharge of the HES while the negative powers from the batteries and supercapacitors represents the power to charge the HES.

Before 8:00, the energy storage system discharges to the load while demand is low. Around 8:00, the demand increases over the threshold (as seen in Fig. 9(a)), the genset reaches the maximum output (6.5 kW). In this case, the engine power can satisfy the load and the additional power is used for charging batteries and super-capacitors, as seen in Fig. 9(c). As the load decreases, more engine power is diverted to charge batteries and super capacitors. The engine does not turn off until the storage system is fully charged and the load goes low. Afterwards, the low load demand is met by the storage discharging until the next peak time comes at 19:00.

TABLE 5. Summary of key performance indicators.

Performance indicator		Spring		Summer		Autumn		Winter	
		proposed	conventional	proposed	conventional	proposed	conventional	proposed	conventional
Energy (kWh)	Electricity from engine	9.59	11.96	9.04	11.01	14.02	16.06	9.57	12.49
	Discharge energy from HES	8.90	-	9.20	-	12.15	-	9.43	-
	Energy for charging HES	6.05	-	6.57	-	9.17	-	5.86	-
	Load consumption	11.96	11.96	11.01	11.01	16.06	16.06	12.49	12.49
Power range (kW)	Load power	[0 to 5.74]	[0 to 5.74]	[0 to 6.1]	[0 to 6.1]	[0 to 9.63]	[0 to 9.63]	[0 to 8.91]	[0 to 8.91]
	Power from engine	[0 to 6.5]	[0 to 6.5]	[0 to 6.5]	[0 to 6.5]	[0 to 6.5]	[0 to 10]	[0 to 6.5]	[0 to 10]
	Power from HES	[-2.71 to 3.51]	-	[-2.71 to 3.02]	-	[-2.71 to 3.15]	-	[-2.71 to 3.27]	-
Duration (hrs)	HES discharge time	20.97	-	21.06	-	20.01	-	21.03	-
	Engine running	3.12	24	2.97	24	4.04	24	3.22	24
	Charge period for HES	3.03	-	2.94	-	3.99	-	2.97	-
	Peak hours	0.09	0.09	0.03	0.03	0.05	0.05	0.25	0.25
Efficiency (%)	HES electric efficiency	19.5	-	16.9	-	21.2	-	17.2	-
	Engine electric efficiency	20.8	3.8	21.2	3.7	22.7	5.2	21.7	4.1
	System electric efficiency	19.7	3.8	17.5	3.7	21.5	5.2	17.8	4.1

The performance indicators for the BDG-HES are listed in Table 5. For the purpose of system evaluation, an engine/gen-set-based conventional power system (CPS) is used as the benchmark. This CPS continuously runs 24 hours every day in order to supply the continuous demands.

1) ENERGY INDICATOR

The load demands for these four days are 11.96 kWh, 11.01 kWh, 16.06 kWh, and 12.49 kWh, respectively. The late autumn and winter days have higher energy needs. Energy demands are satisfied by both of the BDG and the HES in the proposed system while all the energy comes from the engine if CPS is used to the same cases. For the BDG-HES system, take the spring day for example, the energy from the engine is 9.59 kWh; the discharging energy from the storage is 8.9 kWh and that for charging is 6.06 kWh. The total power for the load is: $8.9 + 9.59 - 6.05 = 12.44$ kWh. However, the load consumes 11.96 kWh and the rest is energy loss (0.48 kWh). The energy loss in the rest days are 0.66 kWh, 0.94 kWh, 0.65 kWh respectively.

2) POWER INDICATOR

Power range in different season are different. The peak power is 5.74 kW, 6.1 kW, 9.63 kW and 8.91 kW, respectively. For CPS, it has to satisfy both low power and high power, therefore, an engine with high power capacity is required. By comparison, a 6.5 kW engine/generator is selected for BDG-HES with assistant from HES which can satisfy different power range of demands. The HES has similar charge/discharge power range within these four days which is with maximum charge power of 2.71 kW and with around 3 kW maximum discharge power.

3) TIME INDICATOR

In order to satisfy all the energy demands, an Engine in a CPS has to run 24 hours a day. By contrast, HES takes the main role for energy supply. It discharges in the most day when energy demand keeps low. Discharge period are 20.97 hours, 21.06 hours, 20.01 hours and 21.03 hours, respectively. Engine running period is much lower in a BDG than that in a CPS. They are 3.12 hours, 2.97 hours, 4.04 hours and 3.22 hours, respectively. When an engine running, HES is charged. Charge period are 3.03 hours, 2.94 hours, 4.04 hours and 3.22 hours, respectively. The period of peak demands in these days are quite short, all less than 1 hour.

4) EFFICIENCY INDICATOR

The electric efficiency of the HES in these days range from 16.9% to 21.2%. without assistant of an HES, the CPS has a low efficiency. This was 3.8%, 3.7%, 5.2% and 4.2% for these four days from the calculations while engine efficiency in BDG is 20.8%, 21.2%, 22.8% and 21.8%, respectively. By operating the BDG-HES system with the DP strategy, the efficiency of the proposed system is higher by 19.7%, 17.5%, 21.5%, 17.8% than the CPS over the four days. Clearly, the engine in the BDG-HES works only a limited period while the HES operates over low demand periods.

V. CONCLUSION

This paper has presented a DP-based operational scheme for a bio-fuel-based power generation system with hybrid energy storage. The analytical model is developed based on the bio-engine tests. By the DP algorithm, the energy system is regulated to achieve high efficiency and better energy storage use. The findings can be summarised as follows:

1) The results prove that the methodology developed in this study has improved the system efficiency. Actual demands fluctuated over the four days. But the gen-set would need to switch on two or three times and operate no more than 4 hours per day. This will significantly improve the system efficiency.

2) The engine efficiency is also improved. During the operating period, the loads are levelled by the energy storage system so as to maintain the engine to operate it optimal condition.

3) By the DP optimization scheme, the battery discharging at relatively low power and putting less stress on the batteries

so as to improve both the state of heath and the efficiency of the batteries.

4) The supercapacitor module shows fast response to the power demand and can assist batteries in transient changes.

5) The system efficiency of the proposed system is much higher than a conventional gen-set power system. The developed technologies can be applied to both standalone and grid-tied power network. This will encourage the uptake of bio-energy in power generation.

REFERENCES

[1] P. C. Loh, D. Li, Y. K. Chai, and F. Blaabjerg, "Autonomous control of interlinking converter with energy storage in hybrid AC–DC microgrid," *IEEE Trans. Ind. Appl.*, vol. 49, no. 3, pp. 1374–1382, May/Jun. 2013. doi: 10.1109/TIA.2013.2252319.

[2] S. Mojtahedzadeh, S. N. Ravadanegh, and M.-R. Haghifam, "Optimal multiple microgrids based forming of greenfield distribution network under uncertainty," *IET Renew. Power Gener.*, vol. 11, no. 7, pp. 1059–1068, May 2017. doi: 10.1049/iet-rpg.2016.0934.

[3] Department for Business, Energy & Industrial Strategy. (May 2017). *Energy Trends: Renewables*. Accessed: May 4, 2017. [Online]. Available: https://www.gov.uk/government/uploads/system/uploads/attachment_data/file/604105/Renewables.pdf

[4] P. Prakash and D. K. Khatod, "Optimal sizing and siting techniques for distributed generation in distribution systems: A review," *Renew. Sustain. Energy Rev*, vol. 57, pp. 111–130, May 2016.

[5] W. L. Theo, J. S. Lim, W. S. Ho, H. Hashim, and C. T. Lee, "Review of distributed generation (DG) system planning and optimisation techniques: Comparison of numerical and mathematical modelling methods," *Renew. Sustain. Energy Rev.*, vol. 67, pp. 531–573, Jan. 2017.

[6] Y. Tan, L. Meegahapola, and K. M. Muttaqi, "A review of technical challenges in planning and operation of remote area power supply systems," *Renew. Sustain. Energy Rev*, vol. 38, pp. 876–889, Oct. 2014.

[7] R. J. Best, J. M. Kennedy, D. J. Morrow, and B. Fox, "Steady-state and transient performance of biodiesel-fueled compression-ignition-based electrical generation," *IEEE Trans. Sustain. Energy*, vol. 2, no. 1, pp. 20–27, Jan. 2011. doi: 10.1109/TSTE.2010.2085458.

[8] Y. Wang, F. Ronilaya, X. Chen, and A. P. Roskilly, "Modelling and simulation of a distributed power generation system with energy storage to meet dynamic household electricity demand," *Appl. Therm. Eng.*, vol. 50, no. 1, pp. 523–535, Jan. 2013.

[9] S. Montoya-Bueno, J. I. Muoz, and J. Contreras, "A stochastic investment model for renewable generation in distribution systems," *IEEE Trans. Sustain. Energy*, vol. 6, no. 4, pp. 1466–1474, Oct. 2015. doi: 10.1109/TSTE.2015.2444438.

[10] Y. Li *et al.*, "Optimal stochastic operation of integrated low-carbon electric power, natural gas, and heat delivery system," *IEEE Trans. Sustain. Energy*, vol. 9, no. 1, pp. 273–283, Jan. 2018. doi: 10.1109/TSTE.2017.2728098.

[11] H. Alharbi and K. Bhattacharya, "Stochastic optimal planning of battery energy storage systems for isolated microgrids," *IEEE Trans. Sustain. Energy*, vol. 9, no. 1, pp. 211–227, Jan. 2018. doi: 10.1109/TSTE.2017.2724514.

[12] M. Uzunoglu, O. C. Onar, and M. S. Alam, "Modeling, control and simulation of a PV/FC/UC based hybrid power generation system for stand-alone applications," *Renew. Energy*, vol. 34, no. 3, pp. 509–520, Mar. 2009.

[13] A. Pérez-Navarro *et al.*, "Experimental verification of hybrid renewable systems as feasible energy sources," *J. Renew. Energy*, vol. 86, pp. 384–391, Feb. 2016.

[14] S. Kohsri *et al.*, "Design and preliminary operation of a hybrid syngas/solar PV/battery power system for off-grid applications: A case study in Thailand," *Chem. Eng. Res. Des.*, vol. 131, pp. 346–361, Mar. 2018.

[15] G. C. Seeling-Hochmuth, "A combined optimisation concet for the design and operation strategy of hybrid-PV energy systems," *Sol. Energy*, vol. 61, no. 2, pp. 77–87, Aug. 1997.

[16] E. Krausen and D. Mertig, "Sewage plant powered by combination of photovoltaic, wind and biogas on the island of Fehmarn, Germany," *Renew. Energy*, vol. 1, no. 5, pp. 745–748, Jan. 1991.

[17] E. Unamuno and J. A. Barrena, "Hybrid ac/dc microgrids—Part I: Review and classification of topologies," *Renew. Sustain. Energy Rev.*, vol. 52, pp. 1251–1259, Dec. 2015.

[18] E. Unamuno and J. A. Barrena, "Hybrid ac/dc microgrids—Part II: Review and classification of control strategies," *Renew. Sustain. Energy Rev.*, vol. 52, pp. 1123–1134, Dec. 2015.

[19] E. Planas, J. Andreu, J. I. Gárate, I. M. de Alegría, and E. Ibarra, "AC and DC technology in microgrids: A review," *Renew. Sustain. Energy Rev.*, vol. 43, pp. 726–749, Mar. 2015.

[20] W. Ma, X. Xue, and G. Liu, "Techno-economic evaluation for hybrid renewable energy system: Application and merits," *Energy*, vol. 159, pp. 385–409, Sep. 2018.

[21] M. Winter and R. J. Brodd, "What are batteries, fuel cells, and supercapacitors?" *Chem Rev*, vol. 104, no. 10, pp. 4245–4269, Sep. 2004. doi: 10.1021/cr020730k.

[22] J. Cho, S. Jeong, and Y. Kim, "Commercial and research battery technologies for electrical energy storage applications," *Prog. Energy Combustion Sci.*, vol. 48, pp. 84–101, Jun. 2015.

[23] M. Ansarey, M. S. Panahi, H. Ziarati, and M. Mahjoob, "Optimal energy management in a dual-storage fuel-cell hybrid vehicle using multi-dimensional dynamic programming," *J. Power Sources*, vol. 250, pp. 359–371, Mar. 2014.

[24] D. Fuselli *et al.*, "Action dependent heuristic dynamic programming for home energy resource scheduling," *Int. J. Elect. Power Energy Syst.*, vol. 48, pp. 148–160, Jun. 2013.

[25] Z. Song, H. Hofmann, J. Li, X. Han, and M. Ouyang, "Optimization for a hybrid energy storage system in electric vehicles using dynamic programing approach," *Appl. Energy*, vol. 139, pp. 151–162, Feb. 2015.

[26] Y. Xiao and A. Konak, "A genetic algorithm with exact dynamic programming for the green vehicle routing & scheduling problem," *J. Cleaner Prod.*, vol. 167, pp. 1450–1463, Nov. 2017.

[27] T. Yau, L. N. Walker, H. L. Graham, A. Gupta, and R. Raithel, "Effects of Battery Storage Devices on Power System Dispatch," *IEEE Trans. Power App. Syst.*, vols. PAS–100, no. 1, pp. 375–383, Jan. 1981. doi: 10.1109/TPAS.1981.316866.

[28] Q. Wei, G. Shi, R. Song, and Y. Liu, "Adaptive dynamic programming-based optimal control scheme for energy storage systems with solar renewable energy," *IEEE Trans. Ind. Electron.*, vol. 64, no. 7, pp. 5468–5478, Jul. 2017.

[29] X. P. Chen, N. Hewitt, Z. T. Li, Q. M. Wu, X. Yuan, and T. Roskilly, "Dynamic programming for optimal operation of a biofuel micro CHP-HES system," *Appl. Energy*, vol. 208 pp. 132-141, Dec. 2017.

[30] R. Lawson, "A study of the energy usage in domestic UK dwellings to aid the development of domestic combined heat and power(CHP) and micro renewable technologies," Ph.D. dissertation, School Mech. Syst. Eng., Newcastle Univ., Newcastle upon Tyne, U.K., 2010.

[31] X. P. Chen, Y. D. Wang, H. D. Yu, D. W. Wu, Y. Li, and A. P. Roskilly, "A domestic CHP system with hybrid electrical energy storage," *Energy Build*, vol. 55, pp. 361–368, Dec. 2012.

[32] S. Sinha and S. S. Chandel, "Review of software tools for hybrid renewable energy systems," *Renew. Sustain. Energy Rev.*, vol. 32, pp. 192–205, Apr. 2014.

[33] Dassault System AB. (Mar. 2013). *Getting Started With Dymola*. Accessed: Jan. 30, 2018. [Online]. Available: http://www.claytex.com/wp-content/uploads/2010/03/Getting-started-with-Dymola.pdf

XIANG-PING CHEN received the Ph.D. degree in electronic and electrical engineering from the University of Newcastle upon Tyne, U.K., in 2013. She is currently a Research Associate with Cardiff University, U.K. Her research interests include renewable energy, energy management, and energy storage technologies. Her expertise also lies in optimal operation in multi-vector energy systems and their applications in smart grids.

YAO-DONG WANG received the M.Sc. degree from Guangxi University, China, in 1999, and the Ph.D. degree in mechanical engineering from Staffordshire University, U.K., in 2004.

He is a Chartered Engineer and a member of the Institute of Mechanical Engineers, U.K. He is also a Senior Lecturer and an Active Researcher in sustainable, clean, and renewable energy with Newcastle University, U.K. He has published over 150 papers in peer-reviewed journals. His research interests include miller cycle petrol and diesel engines, flameless oxidation to reduce NOx emissions from gas turbine and power plant, biofuel petrol/diesel engine, biofuel trigeneration and cogeneration with energy storage, energy systems such as biomass/coal thermal power stations: coal and biomass combustion and gasification, organic Rankine cycle, renewable energy systems (wind solar, biomass, and water/hydropower), thermal energy management in processing industries, and building energy saving using passive and active methods. He was an invited reviewer for 12 international journals. He was the Section Chair of ten international conferences.

QIN-MU WU received the Ph.D. degree in control engineering from the Huazhong University of Science and Technology, China, in 2007. Since 2010, he has been a Professor in control theory and control engineering with Guizhou University, China. Before joining Guizhou University, he was with Huawei Technologies Co., Ltd., China, as a Key Member of the R&D Research Group. He is an Experienced Researcher in developing the technologies in optimal control strategies for renewable energy systems and their industrial applications.